

Chapter 2

Synthesis and Experimental Techniques

2.1 Introduction

This chapter provides a comprehensive overview of the experimental methods employed in this study, detailing both the sample preparation process and the range of characterization techniques applied. The samples were synthesized using a standard arc melting furnace, ensuring uniform alloying and high-purity composition. Following synthesis, the chapter outlines the working principles and experimental setups of various instruments used to investigate the physical, magnetic, and thermoelectric properties of the prepared systems. Phase purity and structural confirmation were carried out using X-ray diffraction (XRD). Magnetic behavior was analyzed with a Magnetic Property Measurement System (MPMS), while a custom-built setup was employed for precise thermoelectric measurements. Additionally, a Physical Property Measurement System (PPMS) was utilized to probe magnetotransport properties such as the Hall effect and magnetoresistance.

2.2 Material Synthesis Techniques

The synthesis of magnetic topological insulators (MTIs), Weyl semimetals (WSMs), and kagome lattices requires precise control over crystal growth conditions to achieve high-quality materials with desired electronic and magnetic properties. Various solid-state synthesis techniques are employed to tailor structural, electronic, and magnetic characteristics.

2.2.1 Flux method:

Magnetic topological insulators and kagome lattice are synthesized by introducing magnetic dopants (such as Dy, Ni) into MnBi_2Te_4 and Fe_3Sn_2 . The flux method is particularly useful for growing large, high-quality single crystals of MTIs. Bi_2Te_3 is commonly used as a flux due to its low melting point and ability to dissolve other elements for MnBi_2Te_4 . Magnetic dopant Dy is added in precise amounts to induce magnetic properties. Sn is used as flux for Fe_3Sn_2 . The elements are weighed in a specific ratio and placed in a quartz ampoule under vacuum. The ampoule is heated to a high temperature (900–1100°C) to melt the flux and dissolve the precursor materials. The system is slowly cooled (1–2°C per hour) to allow the gradual nucleation of single crystals. During cooling, magnetic impurities incorporate into the topological insulator and kagome lattice, modifying its electronic and magnetic properties. The remaining flux is removed by centrifugation. This procedure produces large, high-quality single crystals with minimal defects. It allows for precise tuning of magnetic impurity concentration for optimal quantum effects. The flux method is a powerful technique for growing magnetic topological insulators and kagome lattice materials with controlled structural, electronic, and magnetic properties. It enables the slow and controlled growth of single crystals, which is essential for studying quantum effects, magnetic interactions, and topological transport phenomena in these materials.

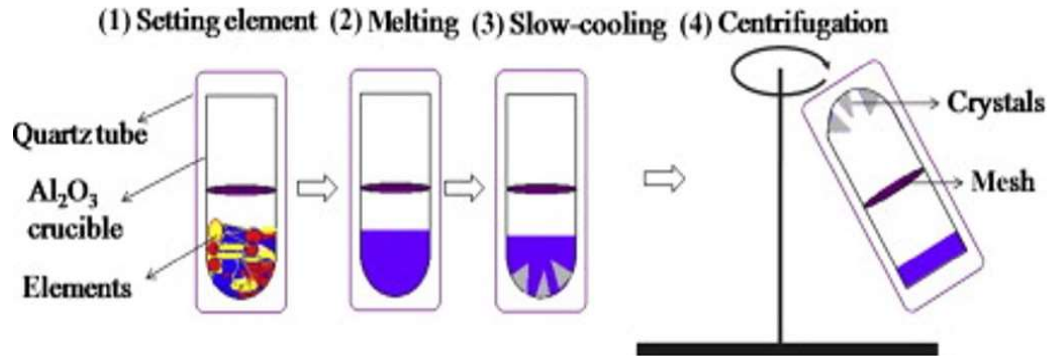


Fig. 2.1 Schematic diagram of sample growth using Flux method (Tsai & Cui (2015)).

2.2.2 Chemical vapour transport:

The single crystal samples of $\text{Nb}_{0.5}\text{Ta}_{0.5}\text{P}$, NbP and TaP were grown in two step process by adhering chemical vapour transport (CVT) technique (Li et al. (2016b)). In first step, we have kept Nb/Ta (99.99% Alfa-Aesar) and P (99.99% Alfa-Aesar) in stoichiometric amount in vacuum sealed quartz ampoule at 950°C for a week, and then furnace cooled slowly to the room temperature. In second step, after examining the phase purity of prepared polycrystalline samples by powder X-ray diffraction (XRD), all the polycrystalline samples were again vacuum sealed in quartz tube with loading of Iodine (13 mg/cm^3) as a transport agent. All the quartz tubes were again placed in the two-zone furnace with creating a temperature gradient by maintaining one zone at 1050°C (sink) and other zone at 950°C (source) for three weeks. Finally, we obtained large polyhedral crystals with dimensions up to 1.0 mm in size, as displayed in inset of Fig. 2.2(b).

2.2.3 Melt Growth Method:

we have synthesized the single crystal of $\text{Bi}_{2x}\text{Gd}_x\text{Se}_3$ (where $x = 0, 0.1$ and 0.16) by modified Bridgeman method (Gangwar et al. (2021); Singh et al. (2020b)). A stoichiometric ratio of high purity Bi (99.99%), Gd (99.99%), and Se (99.99%) was sealed in a evacuated

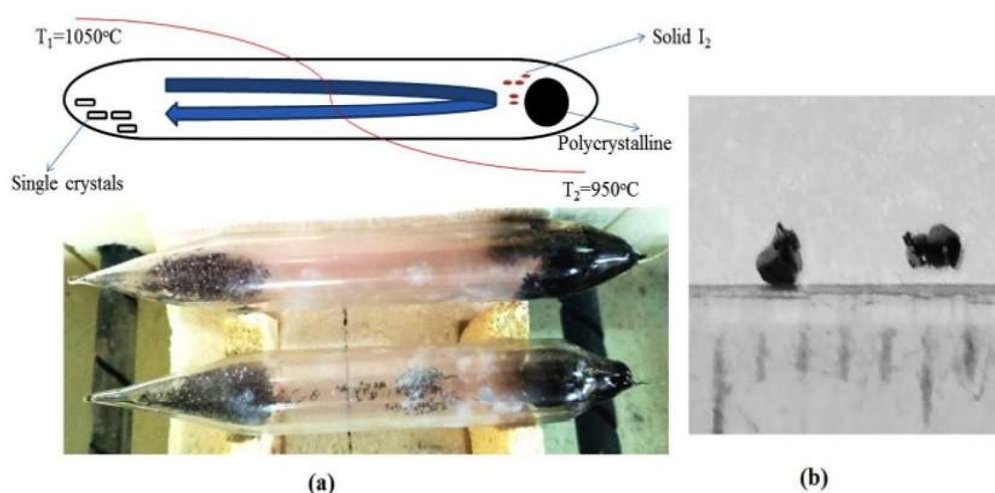


Fig. 2.2 (a) Schematic diagram and sealed quartz tube with iodine for CVT. (b) images of grown samples using CVT method.

quartz ampoule at 10^5 mbar pressure. The temperature of ampoule was ramped upto 900°C at a rate of $200^\circ\text{C}/h$ and was kept at that temperature for 5 hours followed by followed by slow cooling down to 550°C at the rate of $5^\circ\text{C}/h$. Further, it was cooled down to room temperature at the rate of $10^\circ\text{C}/h$. Thus the single crystal was obtained which can be cleaved easily along the plane (00L) direction. The synthesis of MTIs, WSMs, and kagome lattices requires advanced single crystal growth to engineer their quantum properties effectively. These methods enable precise control over magnetic interactions, electronic band structures, and topological phases, essential for realizing next generation quantum materials and spintronic applications.

2.3 Experimental Characterization Tools

2.3.1 X-Ray Diffraction (XRD)

X-ray Diffraction (XRD) is a powerful analytical technique used to study the structure of crystalline materials. It works by directing X-rays at a material and analyzing the way

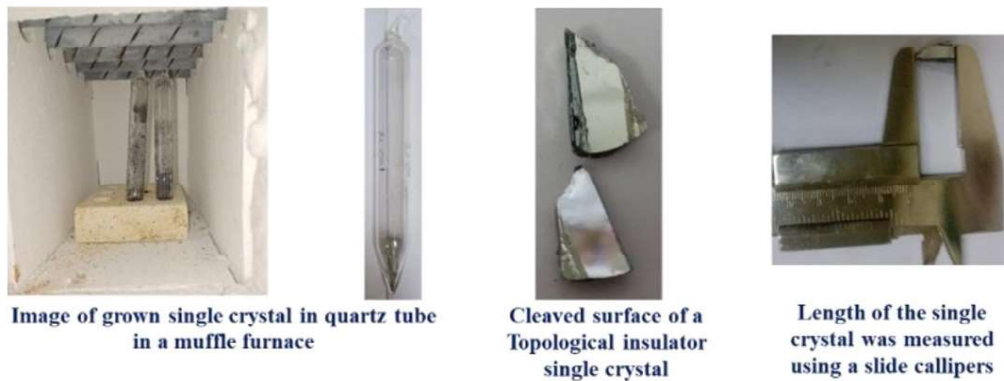


Fig. 2.3 image of growth of crystals in Muffle furnace with temperature controller

these rays are scattered. The scattered rays produce a diffraction pattern, which provides valuable insights into the atomic arrangement within the material. The principle behind XRD is based on Bragg's Law, which relates the wavelength of the X-rays, the angle of incidence, and the spacing between atomic planes in a crystal. When X-rays interact with the electrons in a crystal, they are scattered in various directions. Constructive interference occurs at specific angles, creating a diffraction pattern that is unique to the material's structure. XRD is commonly used to determine the crystal structure, identify unknown materials, measure lattice parameters, and assess the quality of crystalline materials. It is widely applied in fields such as materials science, chemistry, geology, and physics. X-ray Diffraction (XRD) is a powerful analytical technique used to study the structure of crystalline materials. It works by directing X-rays at a material and analyzing the way these rays are scattered. The scattered rays produce a diffraction pattern, which provides valuable insights into the atomic arrangement within the material.

- **Working Principle**

The principle behind XRD is based on Bragg's Law, which relates the wavelength of the X-rays, the angle of incidence, and the spacing between atomic planes in a crystal. When X-rays interact with the electrons in a crystal, they are scattered in various directions.

Constructive interference occurs at specific angles, creating a diffraction pattern that is unique to the material's structure. Bragg's Law is a fundamental principle in X-ray diffraction that helps us understand how X-rays interact with crystalline materials to reveal their atomic structure. It is mathematically expressed as:

$$2d \sin \theta = n\lambda \quad (2.1)$$

n is the order of diffraction, typically an integer, λ is the wavelength of the X-rays, d is the distance between the planes of atoms in the crystal and θ is the angle of incidence at which constructive interference occurs (Pope (1997)). When X-rays hit a crystal, they are reflected off parallel planes of atoms. If the path difference between rays reflected from adjacent planes is an integer multiple of the wavelength ($n\lambda$), constructive interference takes place, producing a detectable diffraction peak. This condition is described by Bragg's Law. Bragg's Law is crucial for determining the crystal structure of materials. By analyzing the diffraction pattern, scientists can calculate the spacing between atomic planes (d) and gain insights into the material's arrangement. Consider X-rays incident on a crystal, which can be imagined as layers of atoms arranged in parallel planes. The X-rays are scattered by atoms in two adjacent planes, separated by a distance d (the interplanar spacing). The angle of incidence and reflection is θ . When X-rays are scattered by atoms in adjacent planes, the path difference between the rays is determined by the extra distance one ray travels compared to the other. This extra path consists of two segments. The ray travels $d \sin \theta$ down to the lower atomic plane. The ray travels another $d \sin \theta$ upward after reflection. Hence, the total path difference is $2d \sin \theta$. Constructive interference occurs when the path difference is an integer multiple of the wavelength. Mathematically, this condition is written as, n is the diffraction order, representing the integer multiples of the wavelength. The equation $n\lambda = 2d \sin \theta$ is Bragg's Law. It relates the X-ray wavelength, the angle of incidence θ , and the interplanar spacing d . By measuring the diffraction angle

θ , one can calculate d to determine the crystal structure. This derivation is pivotal in X-ray crystallography, allowing scientists to analyze crystalline structures explained in Fig. 2.4.

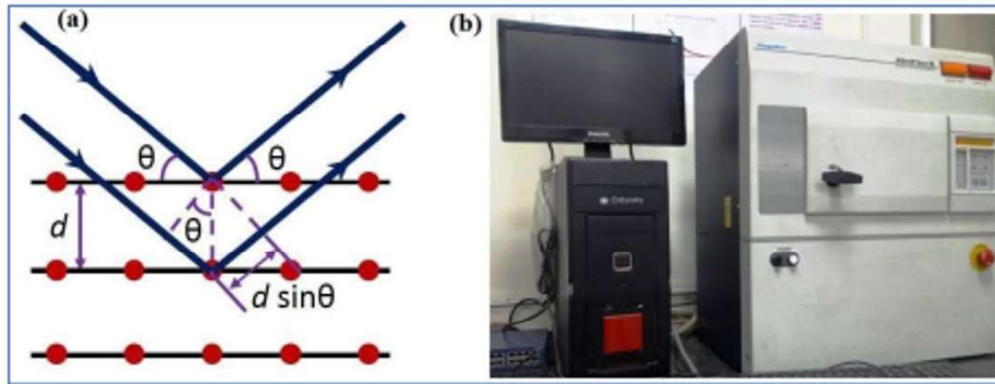


Fig. 2.4 X-ray Diffraction (a) ray diagram and (b) setup

To carry out this measurement, the Rigaku-Miniflex II DESKTOP powder X-ray diffractometer, depicted in figure 2.4, was employed. This diffractometer features a monochromatic X-ray source emitting Cu-K α radiation ($\lambda = 1.5418 \text{ \AA}$) at 30 kV and 15 mA. The recorded data provides valuable insights into the intensity variation with the Bragg angle, aiding in the analysis of the crystalline structure and interatomic distances in the studied material.

2.3.2 Energy Dispersive X ray Spectrum:

The Energy Dispersive X-ray Spectroscopy (EDS or EDX) is a widely used analytical technique for determining the elemental composition of materials. It operates based on the principle of X-ray emission following electron beam interaction with a sample, which leads to the excitation and relaxation of atomic electrons. The emitted X-rays have characteristic energies unique to each element, allowing for qualitative and quantitative analysis shown in Fig. 2.5.

- **Working Principle**

The process begins with the interaction of a high-energy electron beam with the atoms in a sample, typically inside a Scanning Electron Microscope (SEM) or Transmission Electron Microscope (TEM). The incident electrons transfer energy to the atoms, causing the ejection of tightly bound electrons from the inner shells, such as the K-shell or L-shell. This creates an unstable electron vacancy in the atom, leading to a transition where an electron from a higher energy level moves down to fill the vacancy. The energy difference between the two electronic states is released as an X-ray photon, which has an energy characteristic of the specific element. These emitted X-rays are then detected using a Silicon Drift Detector (SDD) or, in older systems, a Lithium-drifted Silicon [Si(Li)] detector. The detector consists of a silicon crystal with a high-purity active region that absorbs the incoming X-ray photons. When an X-ray photon strikes the detector, it ionizes silicon atoms, creating electron-hole pairs proportional to the energy of the absorbed photon. An applied bias voltage sweeps the charge carriers toward an amplifier, where the electrical signal is processed. The number of charge carriers corresponds directly to the energy of the X-ray photon, enabling the system to identify the element that emitted it. After the signal is processed, the data is displayed as a spectrum of X-ray intensity versus energy. Each element present in the sample produces characteristic peaks at specific energies, which are identified by comparing them with a reference database. The height and area of the peaks provide qualitative and quantitative information, indicating the relative abundance of elements in the sample. Since each element has a unique X-ray emission fingerprint, this allows for precise material characterization. EDS is advantageous due to its non-destructive nature, fast data acquisition, and ability to analyze multiple elements simultaneously. It is widely used in materials science, metallurgy, semiconductors, geology, and forensic investigations. However, it has limitations, such as difficulty in detecting light elements below atomic number five (hydrogen, helium, lithium), limited energy resolution, and potential peak overlaps for elements with similar X-ray energies. Overall, EDS is a

fundamental tool in scientific research and industrial applications for elemental analysis. The combination of EDS with electron microscopy techniques provides valuable insights into the composition and microstructure of materials at high spatial resolutions.

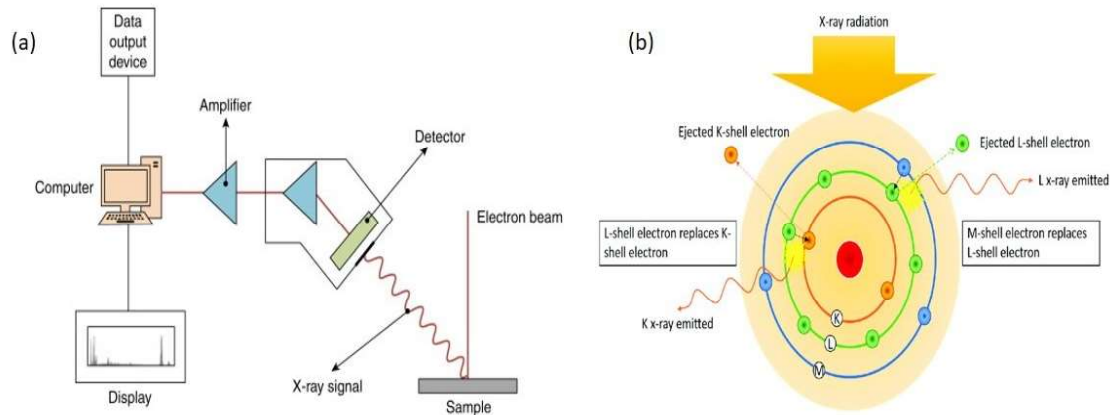


Fig. 2.5 (a) Schematic diagram of Energy dispersive X-ray spectroscopy. (b) diagram depicting capturing the essence of electron liberation in response to incident photons (<http://yunus.hacettepe.edu.tr/selis/teaching/WEBkmu396/ppt/Presentations2010/EDXandWX.pdf>; 2017.)

2.3.3 High Resolution Transmission Electron Microscopy(HR-TEM):

High-Resolution Transmission Electron Microscopy (HR-TEM) is an advanced imaging technique that allows for the visualization of atomic structures in materials with spatial resolutions on the order of sub-angstroms. It operates based on the interaction of high-energy electrons with an ultrathin sample, producing high-magnification images that reveal atomic arrangements, lattice defects, and crystallographic information.

- **working Principle:**

The process begins with the generation of a highly coherent electron beam in an electron gun, typically using a field emission source for superior brightness and spatial coherence. The emitted electrons are accelerated to high voltages, typically ranging from 100 kV to

300 kV, to achieve the necessary de Broglie wavelength for atomic-resolution imaging. The electron beam is then focused into a fine probe using a series of electromagnetic condenser lenses, ensuring a uniform and controlled illumination of the sample. The sample, which must be extremely thin (usually less than 100 nm) to allow electron transmission, interacts with the incident electron beam. As the electrons pass through the sample, they undergo various interactions, including elastic and inelastic scattering. Elastic scattering, where electrons change direction without significant energy loss, contributes to the formation of high-resolution images, while inelastic scattering results in energy loss and contributes to contrast mechanisms such as electron energy loss spectroscopy (EELS). After passing through the sample, the transmitted electrons are collected and further manipulated by a series of objective lenses. The objective lens is critical in forming an initial magnified image, which is then refined by intermediate and projector lenses before reaching the imaging system. The recorded image is based on the phase contrast principle, where variations in the phase of scattered and unscattered electron waves interfere to produce contrast. This interference results in patterns that reveal the atomic structure of the material. A key feature of HR-TEM is the ability to form high-resolution images through phase contrast imaging. This occurs because electrons exhibit wave-like behavior, and their interactions with the crystal lattice lead to phase shifts in the transmitted electron waves. By precisely controlling lens aberrations and defocus conditions, the interference of these phase-shifted electron waves enhances the visibility of atomic columns, enabling direct imaging of individual atoms in crystalline structures. The final image is recorded using a high-resolution camera, such as a charge-coupled device (CCD) or a direct electron detector, which captures the electron intensity distribution with high sensitivity. Advanced image processing techniques, including Fourier transform analysis and contrast enhancement, allow for further refinement and interpretation of atomic-scale details.

HR-TEM provides unparalleled capabilities in characterizing the atomic structure of materials, including defects, grain boundaries, and interfaces. It is widely used in materials science, nanotechnology, semiconductor research, and biological sciences for studying thin films, nanostructures, and complex crystalline materials. Despite its high resolution, HR-TEM requires precise sample preparation and careful imaging conditions to minimize electron beam damage and artifacts that could affect image clarity.

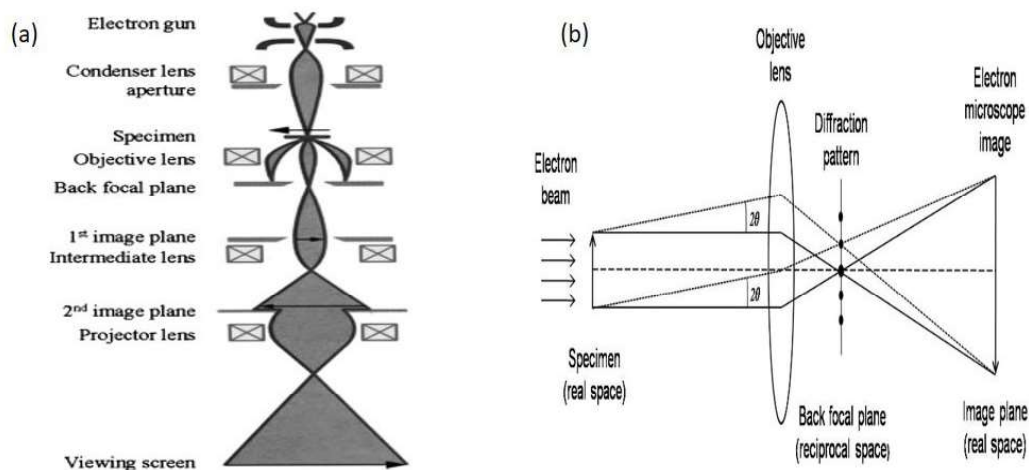


Fig. 2.6 (a, b) Schematic optical diagram of a transmission electron microscope (<https://www.sciencedirect.com/topics/materials-science/high-resolution-transmission-electron-microscopy>.)

2.3.4 X ray Photo Emission Spectroscopy (XPS):

X-ray Photoelectron Spectroscopy (XPS), also known as Electron Spectroscopy for Chemical Analysis (ESCA), is a surface-sensitive analytical technique used to determine the elemental composition, chemical state, and electronic structure of a material. It is based on the photoelectric effect, where incident X-rays excite core electrons in atoms, causing them to be ejected from the material. By measuring the kinetic energy of these emitted electrons, the binding energies of core-level electrons can be determined, providing valuable information about the sample's composition and chemical states.

- **Working Principle**

The process begins with the generation of X-rays, typically from a monochromatic Al $K\alpha$ (1486.6 eV) or Mg $K\alpha$ (1253.6 eV) source. The X-ray beam is directed onto the sample surface in an ultra-high vacuum (UHV) environment to minimize contamination and unwanted interactions with air molecules. When an X-ray photon interacts with an atom in the sample, it transfers its energy to a core electron, typically from the K-shell, L-shell, or M-shell. If the photon's energy is greater than the electron's binding energy, the electron is ejected from the atom in a process known as the photoelectric effect. The ejected electron, now called a photoelectron, travels through the sample and enters the vacuum, where it is collected by an electron energy analyzer. The analyzer measures the kinetic energy of the emitted photoelectron, which is related to the binding energy of the electron by the equation:

$$E_{K.E} = h\nu - (E_B + \phi) \quad (2.2)$$

Here, E_B is the binding energy of the electron, $h\nu$, represents the energy of the incident X-ray photons, $E_{K.E}$ represents the kinetic energy of the electron and ϕ is the work function of the spectrometer. Since the photon energy is known and the work function is a fixed parameter of the instrument, the binding energy of the electron can be accurately determined. Each element has characteristic core-level binding energies, allowing XPS to identify the elements present in the sample. Additionally, shifts in binding energy due to chemical bonding, oxidation states, or coordination environments provide insights into the chemical states of elements. For example, the binding energy of oxygen in metal oxides differs from that in organic compounds, enabling chemical state analysis. The detected photoelectrons originate only from a shallow depth, typically 1–10 nm, due to inelastic scattering losses as electrons travel through the material. This makes XPS highly surface-sensitive, ideal for analyzing thin films, coatings, and surface modifications. Depth profiling can be performed by sputtering the surface with an ion beam, allowing

composition analysis as a function of depth. Besides core-level photoelectrons, XPS spectra also contain Auger electron peaks and satellite features, which provide additional information about electronic structure and chemical bonding. The data is displayed as a spectrum of intensity versus binding energy, with peak fitting and deconvolution techniques used to extract detailed chemical information.

XPS is widely applied in materials science, nanotechnology, catalysis, semiconductors, and surface chemistry to analyze elemental composition, oxidation states, chemical bonding, and contamination. While highly effective, XPS requires ultra-high vacuum conditions, careful sample preparation, and expertise in spectral interpretation to account for peak shifts, background subtraction, and charging effects in insulating materials.

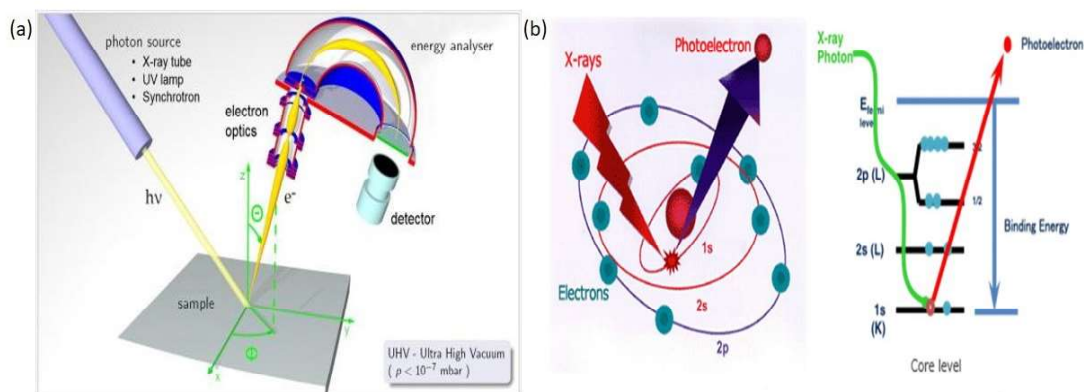


Fig. 2.7 (a) Schematic diagram of XPS setup. (b) Transitions between the core electron from different energy levels (<https://www.ulvac-phi.com/en/surface-analysis/xps>.)

2.3.5 Angle Resolved Photoemission Spectroscopy (ARPES):

Angle-Resolved Photoemission Spectroscopy (ARPES) is a powerful technique used to investigate the electronic structure of materials. It provides direct information about the band structure, Fermi surface, and many-body interactions in condensed matter systems by measuring the energy and momentum of electrons ejected from a sample upon exposure to

ultraviolet (UV) or X-ray photons. ARPES is widely applied in the study of topological insulators, high-temperature superconductors, Weyl semimetals, and strongly correlated electron systems.

- **Working Principle**

The fundamental working principle of ARPES is based on the photoelectric effect. When photons of a known energy ($h\nu$) illuminate the sample, they transfer energy to electrons, which can then overcome the material's work function (ϕ) and be emitted into the vacuum. By analyzing the kinetic energy (E_k) and emission angle (θ) of these photoelectrons, ARPES reconstructs the electronic band structure of the material. The measured kinetic energy of the emitted electron is related to its initial binding energy (E_B) within the material by the equation:

$$E_B = h\nu - (E_k + \phi) \quad (2.3)$$

where E_B represents the binding energy relative to the Fermi level. The emission angle (θ) provides information about the electron's in-plane momentum (k_{\parallel}), given by:

$$K_{\parallel} = \sqrt{\frac{4\pi m E_k}{h}} \sin\theta \quad (2.4)$$

where m is the electron mass and \hbar is the reduced Planck's constant. Since ARPES measures both E_B and k_{\parallel} , it directly maps the band dispersion $E(k)$ revealing the electronic states in momentum space. A typical ARPES setup consists of a photon source, a sample stage in an ultra-high vacuum (UHV) chamber, an electron analyzer, and a detector. The photon source can be a laser, synchrotron radiation, or a gas-discharge lamp, with synchrotron light sources providing tunable photon energies for depth-dependent studies. The sample is precisely aligned and cooled to low temperatures (often below 10 K) to minimize thermal broadening effects and observe subtle features such as superconducting

gaps and topological surface states. The emitted photoelectrons are collected by an energy analyzer, which sorts them by kinetic energy and angle. A two-dimensional detector then records the intensity as a function of energy and momentum, generating ARPES spectra that reveal band dispersions and Fermi surface structures. ARPES is highly sensitive to surface states, as the escape depth of photoelectrons is limited to a few nanometers. However, by varying photon energy, it is possible to probe bulk electronic states as well. In spin-resolved ARPES (SARPES), an additional spin detector allows the measurement of spin polarization, crucial for studying topological insulators and spintronic materials. The technique provides rich insights into fundamental electronic interactions, including electron-phonon coupling, electron correlation effects, and quasiparticle lifetimes. By analyzing band renormalization and energy gaps, ARPES plays a critical role in understanding exotic quantum phases such as charge density waves, Mott insulators, and superconductivity.

Overall, ARPES is an indispensable tool for exploring the electronic properties of advanced materials, enabling a direct visualization of how electrons behave in complex quantum systems. The schematic diagram of ARPES spectra, as illustrated in figure 2.8,

2.3.6 Transport Property Measurements:

Longitudinal Resistivity (ρ_{xx}):

The four-probe method is a widely used technique for measuring the longitudinal resistivity (ρ_{xx}) of a material, particularly at low temperatures and under applied magnetic fields using a Physical Property Measurement System (PPMS). This method eliminates the influence of contact resistance, which is significant in two-probe measurements, ensuring accurate resistivity determination. In this technique, a sample is prepared in a rectangular bar or thin film configuration with four electrical contacts. The contacts are typically made using silver paste, indium, or wire bonding to establish good electrical connectivity. The outer two contacts serve as current electrodes, while the inner two measure the voltage

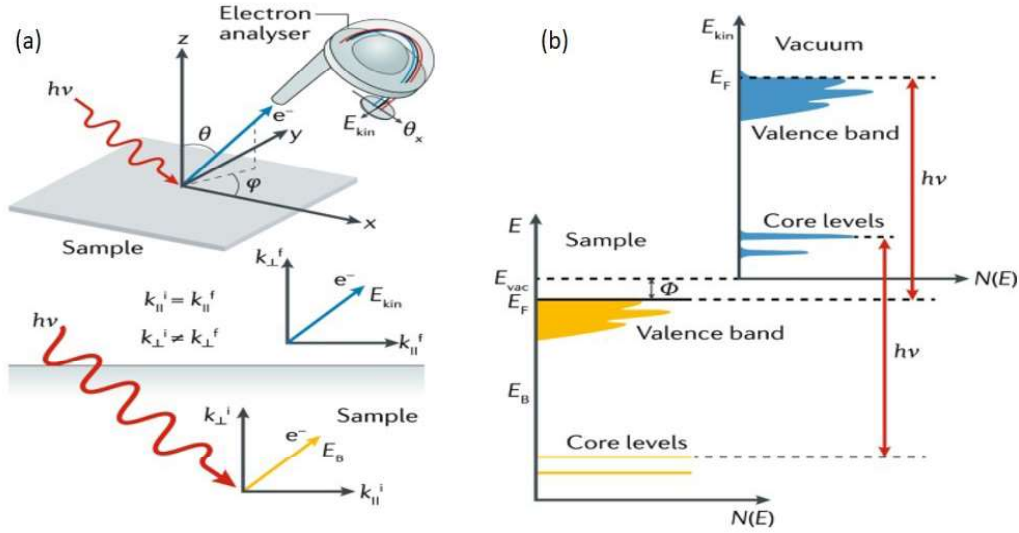


Fig. 2.8 a) Illustration showing the geometry and basic principles of angle-resolved photoemission spectroscopy (ARPES) measurements. b) Energetics of the photoemission process, in which energy is conserved (Lv et al. (2019)).

drop across a defined length of the sample. A precise current (I) is sourced through the outer contacts using a current source, ensuring a uniform flow along the length of the material. The inner voltage contacts measure the potential difference (V) developed due to the current flow. This voltage measurement is done using a high-impedance voltmeter to prevent current draw, ensuring an accurate reading of the potential drop. The longitudinal resistivity (ρ_{xx}) is calculated using Ohm's law and the geometric factors of the sample:

$$R = \frac{V}{I}, \rho_{xx} = \frac{(R \times w)}{t} \quad (2.5)$$

where W is the width of the sample, and t is its thickness. In the PPMS, measurements can be conducted over a broad temperature range, from cryogenic conditions (e.g., 1.8 K) up to room temperature, allowing the study of temperature-dependent transport properties. The applied magnetic field capability in PPMS enables investigation of magnetoresistance effects by measuring resistivity at different field strengths. To minimize experimental errors,

the measurement is often performed using an AC current source with a lock-in amplifier to reduce noise interference. Additionally, a reversal of current polarity is performed to eliminate thermoelectric and background voltage offsets.

The four-probe method in PPMS is crucial for investigating various materials, including semiconductors, topological insulators, and Weyl semimetals, where accurate resistivity measurements are essential for understanding electronic transport mechanisms.

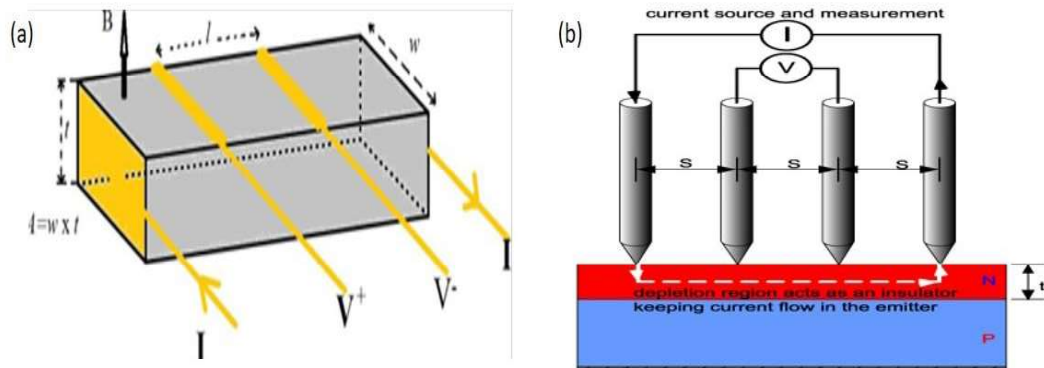


Fig. 2.9 (a) Experimental setup for ρ_{xx} measurement. (b) four probe arrangement for measuring longitudinal resistivity.

Transverse Resistivity (ρ_{xy}):

The four-probe method for measuring transverse resistivity, also known as Hall resistivity (ρ_{xy}), is a widely used technique in the Physical Property Measurement System (PPMS) to study the Hall effect in materials. This method helps determine the charge carrier type, density, and mobility by applying a perpendicular magnetic field to the sample while measuring the transverse voltage.

A sample is typically prepared in a rectangular bar or Hall bar configuration with six electrical contacts. The outermost contacts are used for sourcing the current (I), while the inner voltage probes measure both longitudinal (V_{xx}) and transverse (V_{xy}) voltage. The transverse voltage is measured perpendicular to the applied current direction. A constant

current is supplied along the length of the sample using the outer current contacts. When a perpendicular magnetic field (B) is applied, the Lorentz force acts on the charge carriers, causing them to accumulate on one side of the sample. This accumulation results in a measurable Hall voltage (V_H) across the transverse voltage contacts. The Hall resistivity (ρ_{xy}) is determined using the relation:

$$R_H = \frac{V_H}{IB}, \rho_{xy} = R_H \times t \quad (2.6)$$

Where t is the sample thickness. The Hall coefficient (R_H) provides insight into the charge carrier type as if R_H is positive, the majority carriers are holes (p-type) and if R_H is negative, the majority carriers are electrons (n-type). The carrier concentration (n) can be calculated using:

$$n = \frac{1}{eR_H} \quad (2.7)$$

where e is the elementary charge. Carrier mobility (μ) is obtained from the relation:

$$\mu = \frac{\sigma}{ne} \quad (2.8)$$

where σ is the electrical conductivity. In the PPMS, measurements can be conducted over a wide range of temperatures and magnetic fields to analyze the temperature dependence and field dependence of the Hall effect. To eliminate voltage offsets due to misalignment or thermal effects, measurements are performed by reversing the magnetic field direction (B to $-B$) and averaging the results:

$$V_H = \frac{V(+B) - V(-B)}{2} \quad (2.9)$$

The four-probe Hall measurement method is crucial for studying electronic transport properties in semiconductors, topological insulators, Weyl semimetals, and other materials where charge carrier dynamics play a significant role.

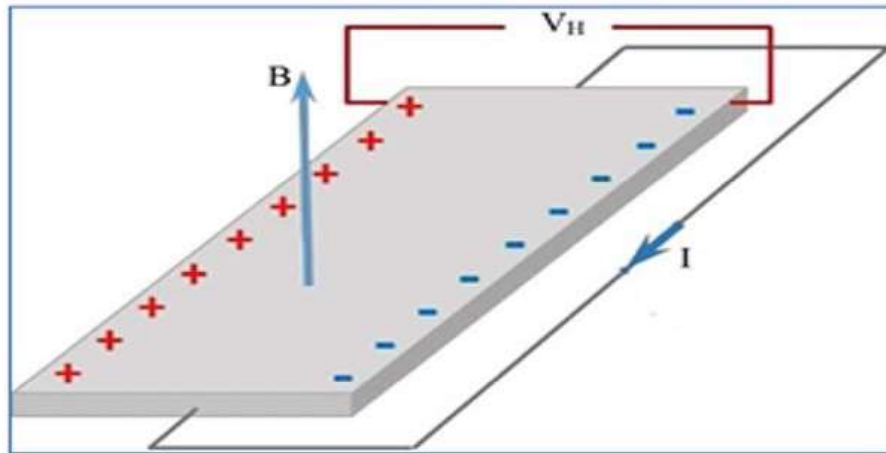


Fig. 2.10 Experimental setup for transverse resistivity measurements.

2.3.7 Thermoelectric Measurements:

The Seebeck coefficient (S) was determined using a custom-built setup, where the sample was sandwiched between two copper blocks. The sample holder assembly was mounted on a closed-cycle refrigerator (CCR), capable of cooling the sample from room temperature down to 20 K in a controlled manner. A temperature difference (ΔT) of 2 K was maintained across the sample using T-type thermocouples, with heater coils placed at both ends of the copper blocks. The voltage difference (ΔV) between the hot and cold ends of the sample was measured using a Keithley 2182A nanovoltmeter over the entire temperature range. The sample holder assembly is illustrated in Figure 2.11. As heat was applied, charge carriers diffused from the hot end to the cold end, generating a thermal current. The Seebeck coefficient (S) is defined as the ratio of the induced thermoelectric voltage (ΔV)

to the temperature difference (ΔT) across the sample:

$$S = \frac{\Delta V}{\Delta T} \quad (2.10)$$

where S is expressed in $\mu\text{V}/\text{K}$. The sign of the Seebeck coefficient provides insight into the nature of charge transport. A negative value indicates n-type conduction (electron-dominated transport), while a positive value suggests p-type conduction (hole-dominated transport).

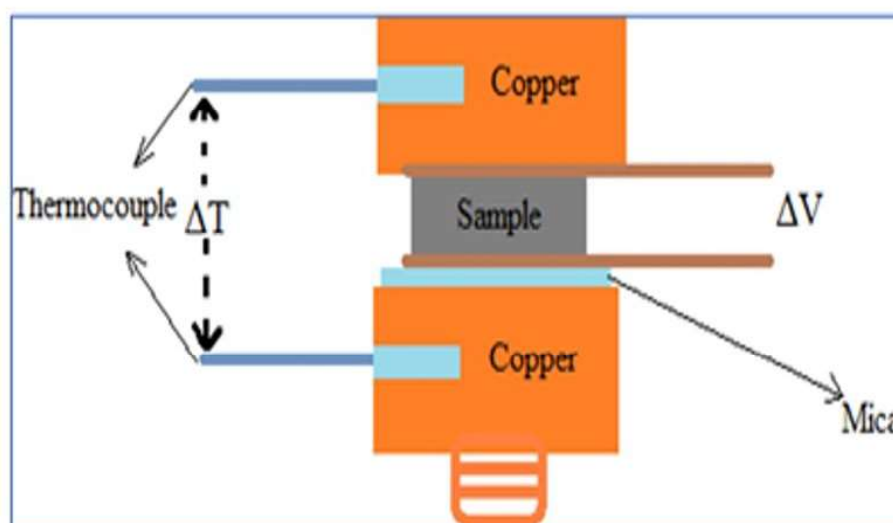


Fig. 2.11 Schematic diagram of sample holder for thermoelectric measurement. Temperature difference at the both ends of the sample creates a temperature gradient.

2.3.8 Magnetic Property Measurement System(MPMS):

A Magnetic Property Measurement System (MPMS) is widely used to measure the magnetization (M) as a function of temperature (M - T) and magnetic field (M - H) using a Superconducting Quantum Interference Device (SQUID). The SQUID sensor provides high sensitivity (down to 10^8 emu) for detecting magnetic signals, making it ideal for

studying weakly magnetic materials, superconductors, and nanomaterials. The MPMS SQUID magnetometer operates based on the following key components and principles:

- Superconducting Quantum Interference Device (SQUID)

It consists of a superconducting loop interrupted by one or two Josephson junctions, which are weak links allowing quantum tunneling of Cooper pairs. The core principle relies on the quantization of magnetic flux within the superconducting loop, meaning that the total magnetic flux is constrained to integer multiples of the flux quantum ($\phi_0 = h/2e$). When an external magnetic field is applied, it induces a change in the flux through the loop, altering the phase difference across the Josephson junctions. This leads to an oscillatory variation in the critical current, which is highly sensitive to even minuscule changes in the magnetic field. By measuring the voltage across the junctions as a function of the applied current, the SQUID can detect variations in magnetic flux with unparalleled precision, down to 10^{15} Tesla. When a sample is placed in a uniform applied magnetic field (H), the magnetic moment (M) of the sample induces a flux change that is detected by the SQUID sensor.

- Superconducting Magnet

The MPMS contains a superconducting solenoid that generates highly stable and uniform magnetic fields, ranging from 0 to ± 7 Tesla (depending on the model). The applied field (H) interacts with the sample, causing a measurable magnetization (M).

- Sample Vibrating Mechanism (VSM Mode)

In modern MPMS systems, a Vibrating Sample Magnetometer (VSM) mode is available. The sample vibrates at a fixed frequency (typically 40 Hz), inducing a time-dependent magnetic flux that is detected by the SQUID.

- Detection Coils (Pickup Coils)

A set of superconducting pickup coils surrounds the sample chamber. The sample is moved along the z-axis (axial direction), and the change in the induced voltage is recorded. This voltage is proportional to the magnetization (M) of the sample.

DC Magnetization and AC Susceptibility Measurements

To study the magnetic properties of a material, both DC magnetization and AC susceptibility measurements are performed using a SQUID-based magnetometer or a vibrating sample magnetometer (VSM) explained in Fig. 2.12. These measurements help analyze phase transitions, magnetic ordering, and dynamical effects in materials. The key measurement protocols include:

- Zero-Field-Cooled Heating (ZFC):

In this protocol, the sample is initially cooled from room temperature down to the lowest measurement temperature without any applied magnetic field. Once the desired temperature is reached, a magnetic field is applied, and the magnetization (M) is recorded while heating the sample to a higher temperature. The ZFC process helps identify the thermal activation of magnetic moments and phase transitions.

- Field-Cooled (FC):

For an FC measurement, the sample is cooled from room temperature to the lowest measurement temperature in the presence of an applied magnetic field. The magnetization (M) is recorded during the cooling process. The FC curve is often compared with the ZFC curve to understand irreversible magnetic behavior, spin glass states, or superparamagnetic relaxation.

- Field-Cooled Heating (FCH):

After completing the FC protocol, the magnetization is measured during the heating process while maintaining the applied magnetic field. This helps detect hysteresis effects and thermal reversibility of magnetic states.

- Magnetization vs. Field (M-H) Measurement:

M-H curves, also known as hysteresis loops, are measured by applying a varying magnetic field at a constant temperature. The field is swept from a negative maximum to a positive maximum and back, allowing the measurement of key magnetic properties such as, Saturation magnetization (M) where the maximum magnetization achieved at high fields. Remanent magnetization (M_r) where the residual magnetization after the field is removed and Coercive field (H_c) where the field required to reduce magnetization to zero. These measurements provide insights into ferromagnetic, antiferromagnetic, and spin-glass behaviors.

- AC Susceptibility (χ' and χ''):

Unlike DC magnetization, AC susceptibility measurements involve applying a small oscillating magnetic field (H_{ac}) and recording the material's response as a function of temperature (T) and frequency (f). The AC susceptibility consists of two components, real part (χ') represents the in-phase response, which corresponds to the reversible magnetization and imaginary part (χ'') represents the out-of-phase response, which is related to energy dissipation and relaxation processes. AC susceptibility is particularly useful for studying magnetic relaxation, spin dynamics, superconducting transitions, and spin-glass freezing. By analyzing the temperature and frequency dependence of χ' and χ'' , one can determine activation energies and critical slowing down in magnetic systems.

This comprehensive approach to DC and AC magnetic measurements allows researchers to explore fundamental magnetic phenomena in various materials, including ferromagnets, superconductors, and topological magnets.

Magnetocaloric effect measurement

The magnetocaloric effect (MCE) is a phenomenon where a material undergoes a temperature change upon the application or removal of a magnetic field. This effect arises due to the coupling between the magnetic and thermal properties of a material. When a magnetic field is applied, the magnetic moments of the atoms align, reducing the material's magnetic entropy. If this process occurs adiabatically (without heat exchange with the environment), the reduction in magnetic entropy is compensated by an increase in lattice entropy, resulting in a temperature rise. Conversely, removal of the magnetic field leads to increased magnetic disorder and a temperature drop. MCE is especially pronounced near magnetic phase transitions, such as the Curie temperature in ferromagnets (Tishin & Spichkin (2016)).

To measure the MCE, key experimental techniques include isothermal magnetization and heat capacity measurements. Isothermal magnetization $M(H, T)$ is recorded at various temperatures around the magnetic transition to calculate the magnetic entropy change (ΔS_M) using the Maxwell relation:

$$\left(\frac{\delta S_M(T, H)}{\delta H}\right)_T = \left(\frac{\delta M(T, H)}{\delta T}\right)_H \quad (2.11)$$

The magnetic entropy change ($\Delta S_M(H)$) for MBT system can be calculated as:

$$\Delta S_M(T, H) = \int_0^H \left(\frac{\delta M}{\delta T}\right) dH \quad (2.12)$$

ΔS_M is the magnetic entropy change, whereas H is the external magnetic field applied to the material (Bai & Xu (2025)).

This is commonly done using a Vibrating Sample Magnetometer (VSM) or SQUID magnetometer. Alternatively, direct MCE measurements can be performed using a calorimeter to monitor temperature changes under varying magnetic fields. For more

comprehensive analysis, heat capacity (C_p) measurements under different magnetic fields can provide the adiabatic temperature change (ΔT_{ad}), giving further insight into the efficiency of a material for magnetic refrigeration applications.

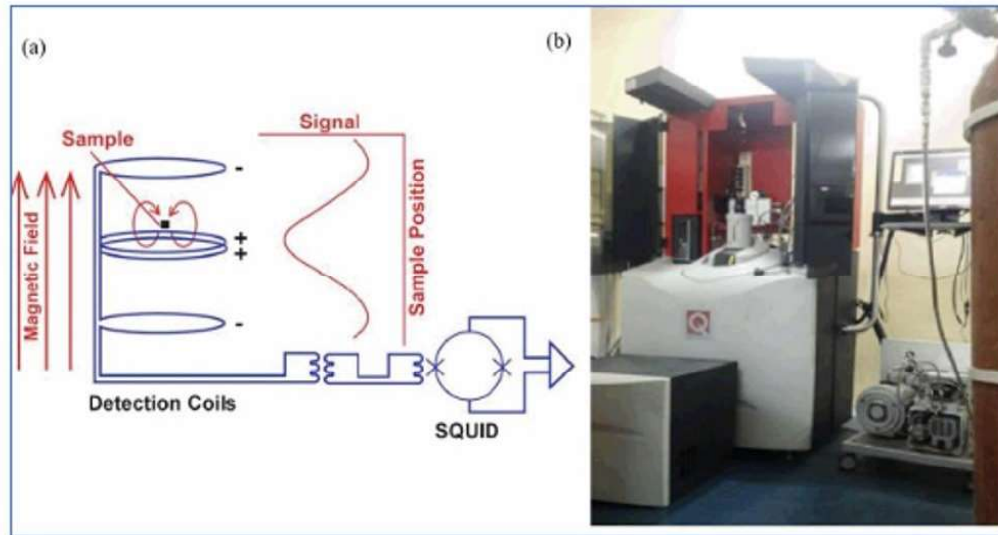


Fig. 2.12 (a) Schematic diagram of SQUID-VSM detection system. (b) Photograph of actual QD-MPMS measurement system (Yildirim (2016)).